Supplementary Information For

Sirt6 regulates TNFα secretion via hydrolysis of long chain fatty acyl lysine

Hong Jiang[1,#], Saba Khan[1,#], Yi Wang[2,#], Guillaume Charron[3], Bin He[1], Carlos Sebastian[4], Jintang Du[1], Ray Kim[1], Eva Ge[1], Raul Mostoslavsky[4], Howard C. Hang[3], Quan Hao[2,*], and Hening Lin[1,*]

[1]Department of Chemistry and Chemical Biology, Cornell University, Ithaca, NY 14853, USA

[2]Department of Physiology, University of Hong Kong, Hong Kong, China

[3]The Laboratory of Chemical Biology and Microbial Pathogenesis, The Rockefeller University, 1230 York Avenue, New York, NY 10065.

[4]The Massachusetts General Hospital Cancer Center, Harvard Medical School, 185 Cambridge St., Boston, MA 02114

[#]These authors contributed equally to this work

*Correspondence should be addressed to H.L. (hl379@cornell.edu) and Q.H. (qhao@hku.hk)

Table S1. Data collection and refinement statistics for Sirt6-myrH3K9-ADPR complex

Data collection	
Space group	R32
Cell dimensions	
a, *b*, *c* (Å)	104.89, 104.89, 231.49
α, β, γ (°)	90, 90, 120
Resolution (Å)	40.00-2.20
R_{sym} or R_{merge} (%)	6.0 (75.2)
$I / \sigma I$	47.94 (4.72)
Completeness (%)	99.8 (100.0)
Redundancy	10.8(11.0)
Refinement	
Resolution (Å)	35.73-2.20
No. reflections	23603
R_{work} / R_{free} (%)	19.11/23.58
No. of protein residues	294
No. of ligand/ion molecules	
Myristoyl H3K9	1
ADPR	1
Glycerol	2
Zn	1
No. of water	168
B-factors	
Protein	42.31
Myristoyl H3K9	61.86
Zn	49.87
Water	45.91
r.m.s. deviations	
Bond lengths (Å)	0.02
Bond angles (°)	2.21

Values in parentheses are from the highest resolution shell

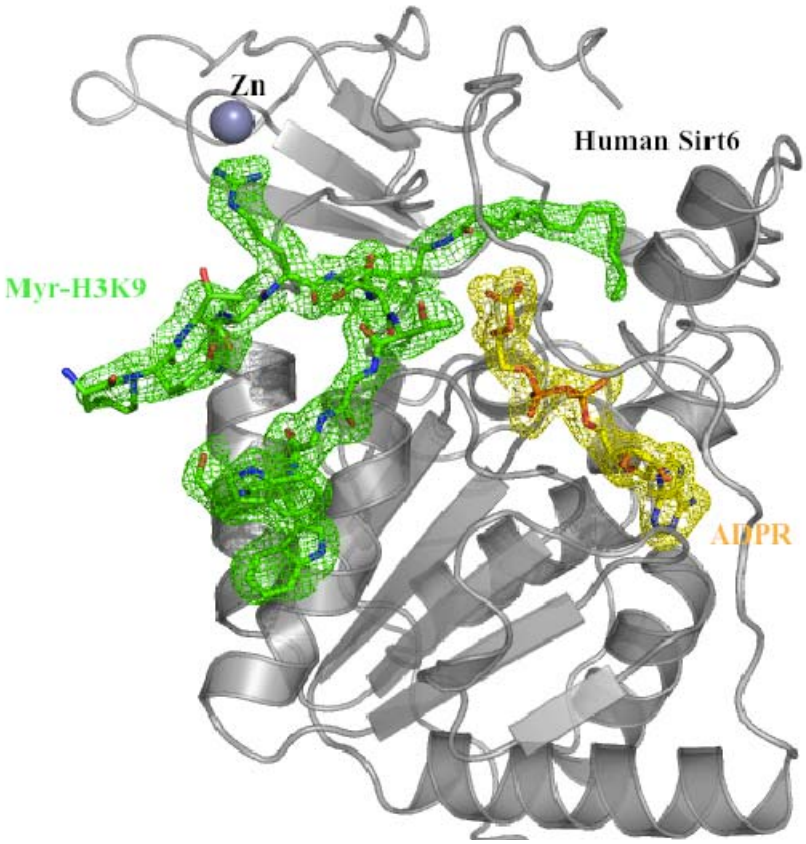

Figure S1. Overall structure of Sirt6 with the 2Fo-Fc omit electron density map at 1σ showing myristoyl lysine (H3K9-Myr, green) peptide and ADP-ribose (ADPR, yellow) bound.

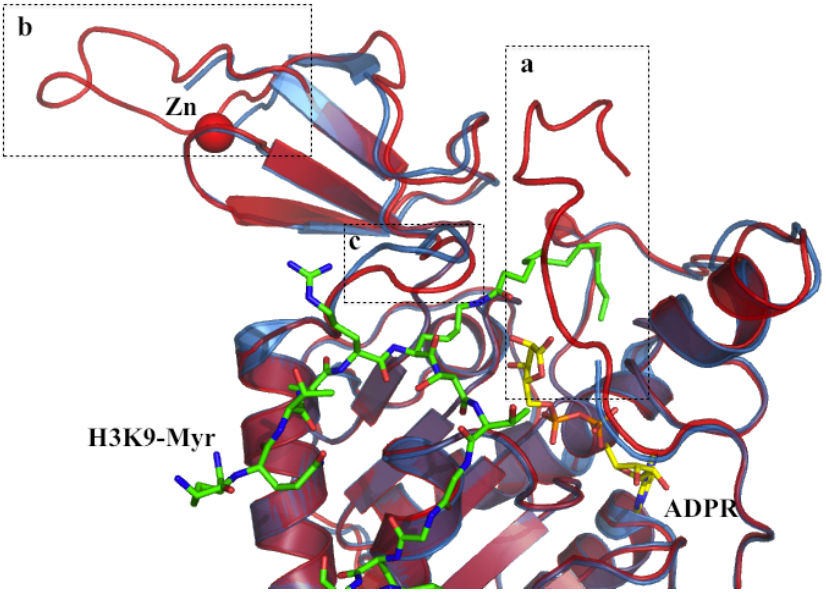

Figure S2. The complex Sirt6 structure colored in red is superimposed with the published apo Sirt6 structure colored in blue (PDB 3K35). Boxes *a* and *b* highlight the N-terminal loop and Zinc binding domain respectively. Box *c* shows the movement of one of the loops upon binding of H3K9-Myr.

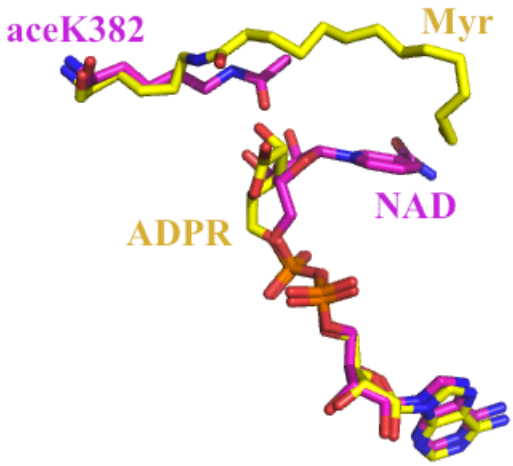

Figure S3. The structural alignment between Sir2Tm (PDB id 2H4F, magenta) and human Sirt6 (yellow) shows that both H3K9-Myr and ADPR in Sirt6 bind similarly to the enzyme as ligand binding in other sirtuins.

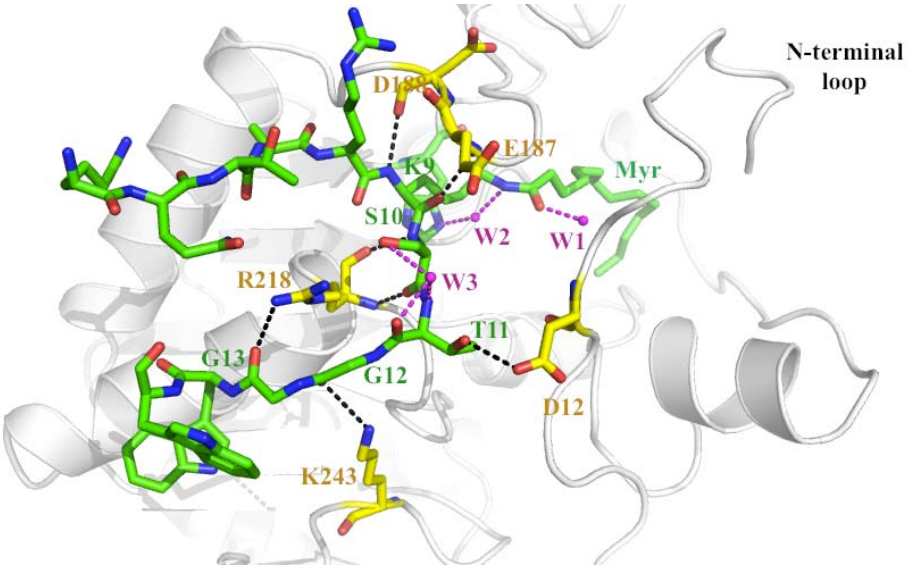

Figure S4. Hydrogen bonding interactions around the H3K9-Myr ligand. Side chains of different amino acids (colored in yellow) on the Sirt6 loops interact with and stabilize the H3K9-Myr peptide (colored in green). Three water molecules, W1, W2 and W3 (colored in purple) also help stabilize the peptide via hydrogen bonds.

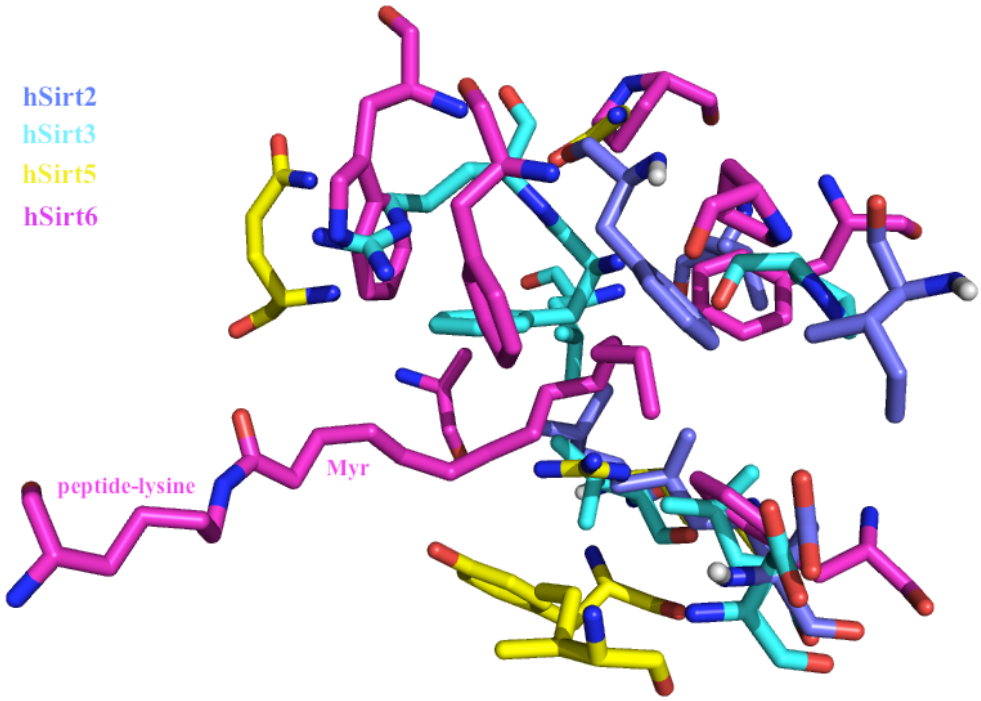

Figure S5. Substrate-binding pocket comparison between Sirt6 (magenta) and other human sirtuin structures (Sirt2, PDB id 1J8F, purple; Sirt3, PDB id 3GLS, cyan; Sirt5, PDB id 3RIY, yellow). The myristoyl group in the Sirt6 structure would be too long to fit into the pocket of Sirt2, Sirt3 or Sirt5.

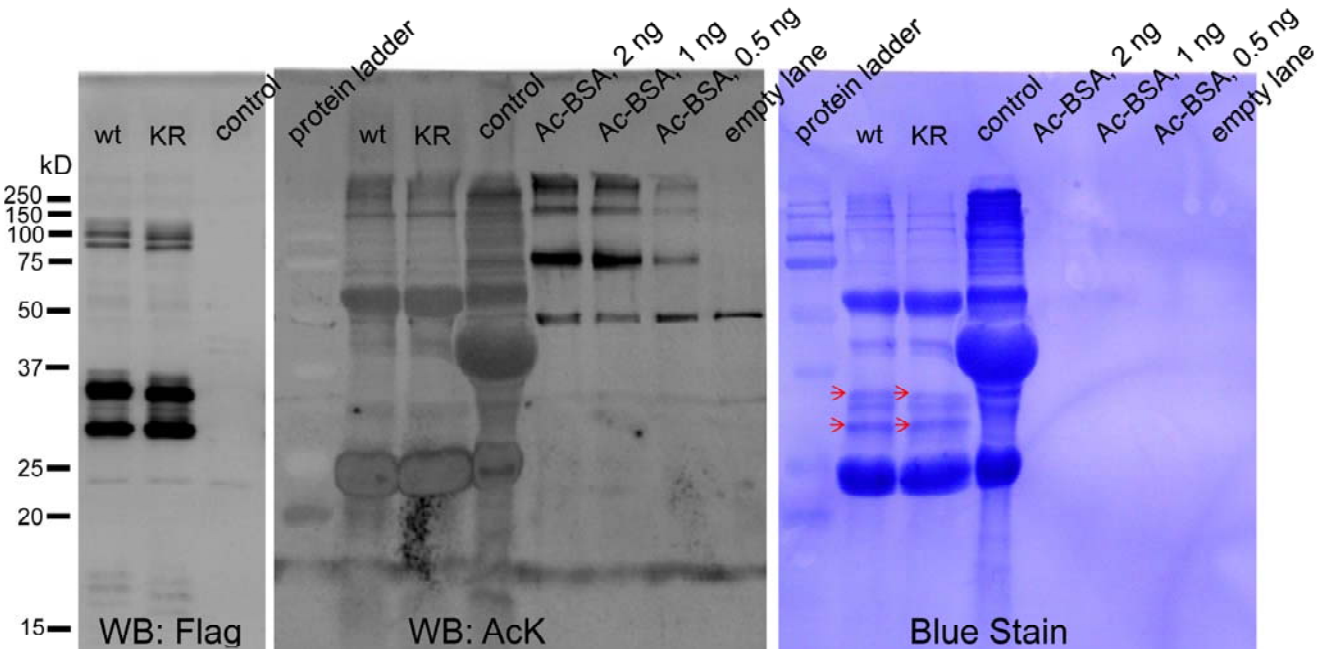

Figure S6. No acetylation was detected on TNFα by Western blot. The pCMV vectors containing Flag-tagged TNFα were transiently transfected into Sirt6 knockout MEF cells. The empty pCMV vector was used as a control. The left panel was the Western blot for Flag to show the expression of TNFα wild type (wt) and K19/K20 to Arg mutant (KR). Middle panel was the Western blot using a pan-specific acetyl lysine antibody and the right panel was the same Western blot membrane with Coomassie blue staining. Red arrows point out TNFα protein positions. No difference in the acetylation level on TNFα wt and KR was observed. Acetylated BSA was used as the control for acetylated proteins.

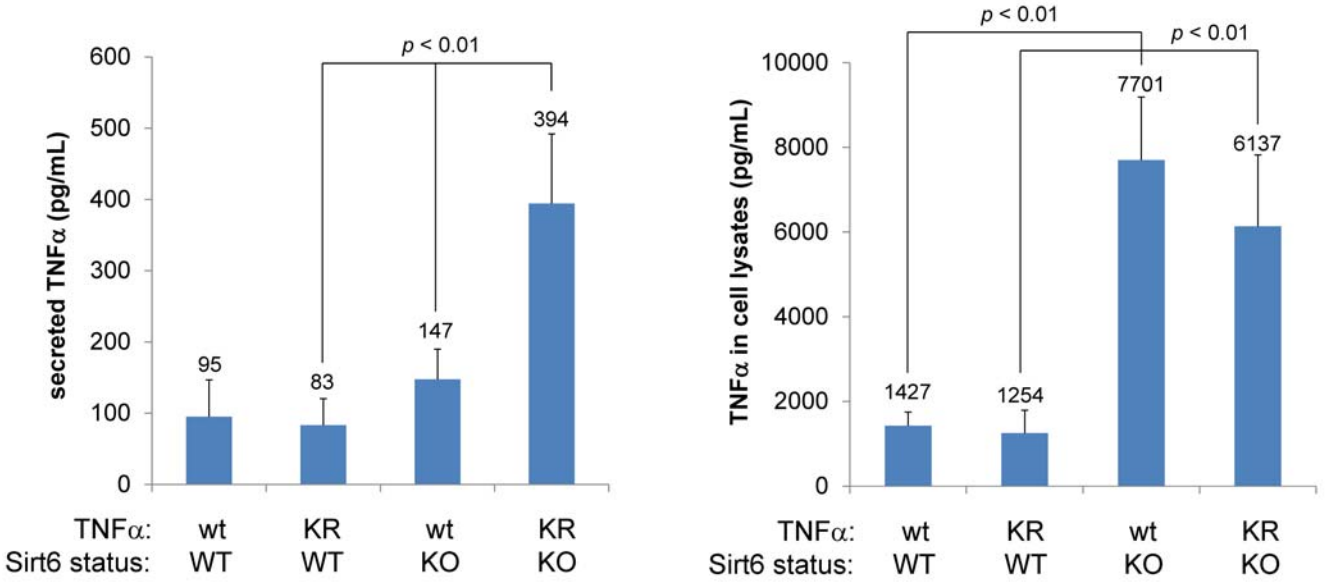

Figure S7. TNFα level in culture medium (total 10 mL for each sample) and cell lysates (total 0.26 mL for each sample) of Sirt6 WT/KO cells (transient transfected with human TNFα wt or KR mutant). Each data point is the average of six independent experiments. These data were used to calculate the secretion efficiency shown in Figure 3E. The amounts of TNFα are different in different cell lines probably because of the variation in the number of cells used (Sirt6 KO cells grow much faster than Sirt6 WT cells)

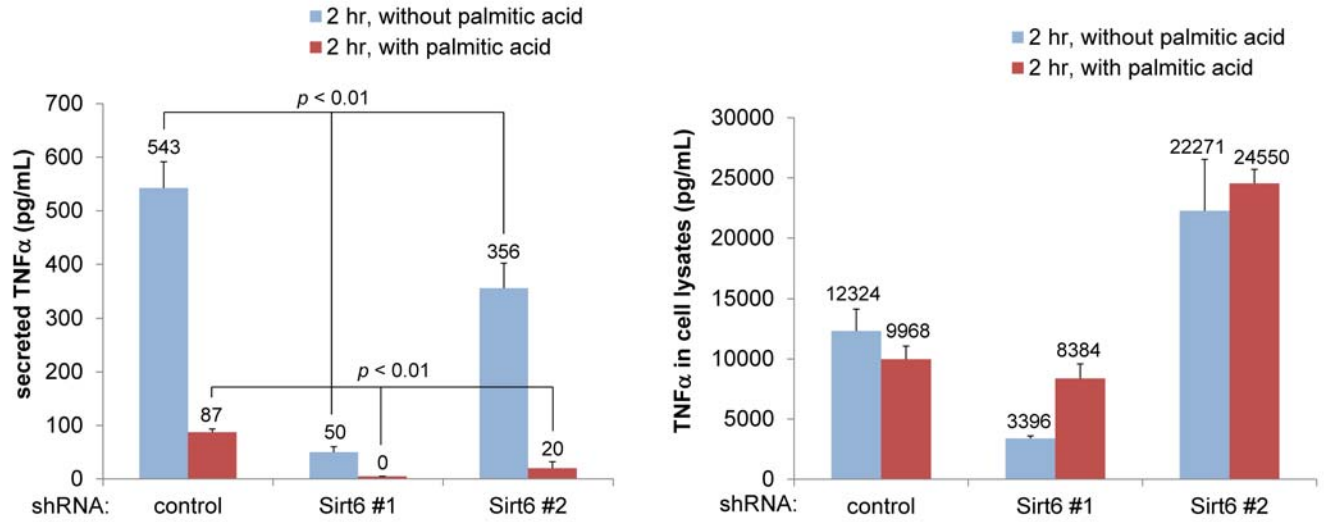

Figure S8. TNFα level in culture medium (total 30 mL for each sample) and cell lysates (total 0.245 mL for each sample) of THP-1 cells (infected with control shRNA, Sirt6 shRNA #1 and #2). Each data point is the average of three independent experiments.

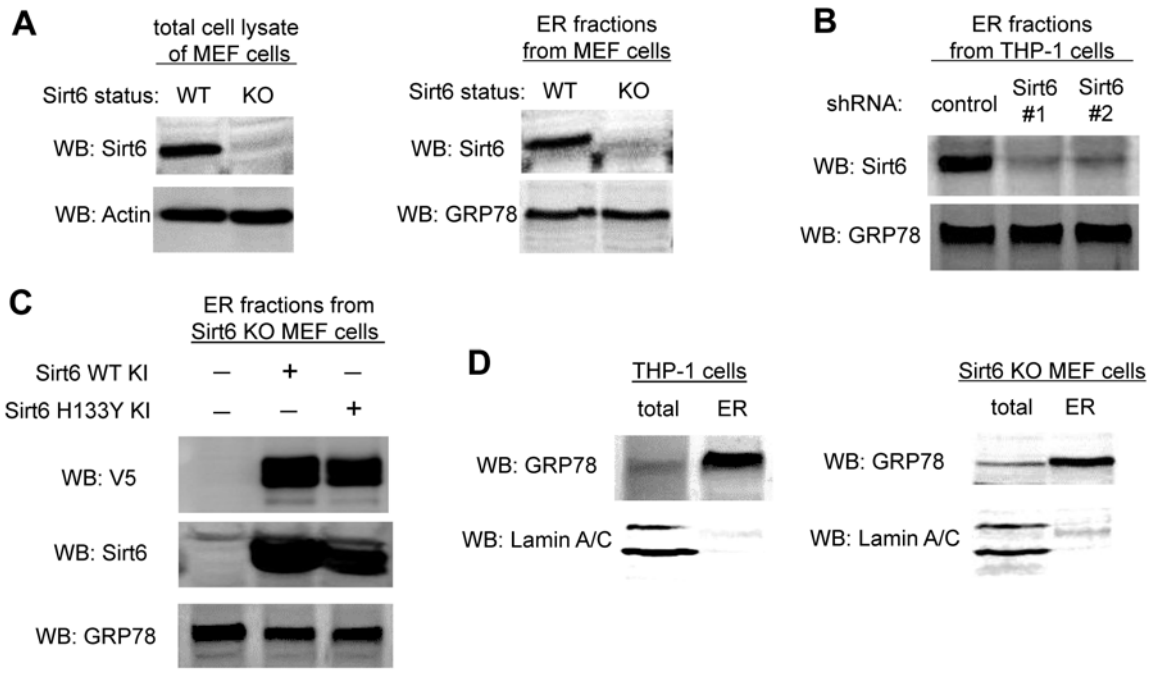

Figure S9. Sirt6 exists in ER. (A) Endogenous Sirt6 was detected in ER fraction from Sirt6 WT MEF cells but not in Sirt6 KO MEF cells. Actin was used as loading control for total cell lysate. GRP78, an ER marker was used as loading control for ER fraction. (B) Endogenous Sirt6 was detected in ER fraction from control shRNA THP-1 cells, while less Sirt6 was detected in ER fractions from Sirt6 shRNA #1 or #2 THP-1 cells. GRP78 was used as the loading control. (C) Exogenous human Sirt6 was detected in ER fractions from Sirt6 KO MEF cells. Exogenous human Sirt6 WT and H133Y mutant have C-terminal V5 tag. GRP78 as an ER marker was used as loading control. (D) ER fractions were blotted for GRP 78 (ER marker) and Lamin A/C (nucleus marker) to demonstrate that the ER fractions were not contaminated by nuclear protein Lamin A/C.

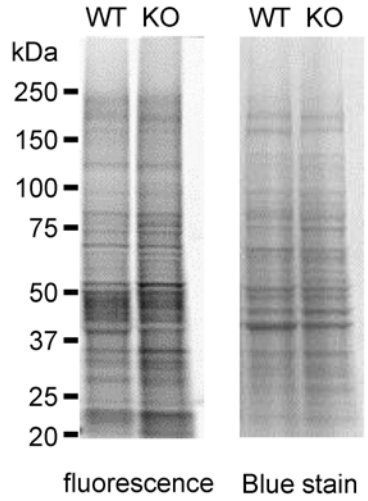

Figure S10. Alk14 labeling of Sirt6 WT and KO MEF cell lysates. Left image shows the fluorescent signal (fatty acylation level) and right image shows Coomassie blue stained protein gel. WT and KO cell lysates had roughly similar amount of proteins, but several proteins showed higher fatty acylation level in Sirt6 KO MEF cells than in WT MEF cells, suggesting that Sirt6 may regulate the fatty acylation level of other proteins.